minerals

Article

Geochemical Characteristics of Critical Metal Elements in the No. 9 Coal Seam from the Xinyuan Mine, Northern Qinshui Coalfield, Shanxi Province, China

Jian Li [1,2,3,*], Shaowei Zhang [1,2,3], Hongdong Wang [1,2,3] and Xichao Xie [1,2,3]

1 Shanxi Institute of Geology and Mineral Resources Company Limited, Taiyuan 030001, China
2 Shanxi Key Laboratory of Coal and Coal-Measure Gas Geology, Taiyuan 030024, China
3 Provincial Center of Technology Innovation for Coal Measure Gas Co-Production, Taiyuan 030001, China
* Correspondence: lijianyjs@126.com

Abstract: As one of the main fossil fuels globally, coal can be enriched with a variety of critical metal elements in specific geological conditions. This paper investigates the mineral compositions and concentrations of major and minor element oxides and trace elements in the No. 9 coal from the Xinyuan mine of the northern Qinshui coalfield, China, and discusses the modes of occurrence and enrichment mechanisms of critical metal elements such as Li, Ga, Th and REY. The mineral compositions of the No. 9 coal are primarily represented by clay minerals and quartz, with a small amount of calcite, siderite, anatase, etc. The major element oxides in the No. 9 coal are dominated by SiO_2 and Al_2O_3. Compared with world hard coal, the No. 9 coal of the Xinyuan mine is rich in Li (CC = 8.00) and Th, slightly enriched with Pb, Sc, Ga, Y, La, Ce, Tb, Dy, Er, Yb and Hg, and depleted in Mn, Co, Ni, Rb, Cs and Tl. The critical metal elements such as Li, Ga, Th and REY that enriched No. 9 coal mainly occur in aluminum silicates. The genetic type of the critical metal elements in the No. 9 coal from the Xinyuan mine is source rock-controlled type. The critical metal minerals and solutions from the source area were transported to the study area by the action of water. Due to the change of swamp water conditions, the critical metal elements were combined with clay minerals and enriched the coal.

Keywords: critical metal elements; trace elements; lithium enrichment; Qinshui coalfield; Xinyuan mine

check for updates

Citation: Li, J.; Zhang, S.; Wang, H.; Xie, X. Geochemical Characteristics of Critical Metal Elements in the No. 9 Coal Seam from the Xinyuan Mine, Northern Qinshui Coalfield, Shanxi Province, China. *Minerals* **2023**, *13*, 278. https://doi.org/10.3390/min13020278

Academic Editors: Thomas Gentzis, Xiaomei Wang, Shuqin Liu and Lei Zhao

Received: 29 December 2022
Revised: 5 February 2023
Accepted: 10 February 2023
Published: 16 February 2023

1. Introduction

Critical metals and mineral resources play an irreplaceable and important role in new materials, new energy, information technology, and the aerospace industry [1]. As one of the main fossil fuels globally, coal can be enriched with a variety of beneficial elements, including critical metal elements (e.g., Li, Sc, V, Ga, Ge, Se, Y and rare earth elements, Zr, Nb, Au, Ag, and platinum group elements, Re, and U [2]), in specific geological conditions [2–4], and can form 'coal-hosted rare metal deposits' or 'metalliferous coal' [5,6].

Coal-hosted critical metal elements are an important direction in the study of coal geology and mineral deposits. In recent years, researchers from the United States [7,8], Europe [9–11], Russia [12,13], South Africa [14] and China [15–18] have all conducted research in this field and achieved a set of high-level research results. The Qinshui coalfield is an important lean coal and anthracite base in Shanxi Province, and it is also one of the most important areas for coalbed methane exploration and exploitation. In terms of the research on critical metal elements, Zhao et al. [19,20] systematically studied the distribution and enrichment origin of critical metals such as Li, and rare earth elements in the coal from Jincheng mining area in the southeastern Qinshui coalfield. Wang et al. [21] studied the distribution characteristics of rare earth elements in coal from the Qinshui coalfield. Hou et al. reported the latest data on the petrology, mineralogy, and coal geochemistry of the No. 15 coal seam in the southeastern Qinshui basin [22]. However, there is little research on critical metals from the northern Qinshui coalfield. In this study, we investigate the mineralogical and geochemical characteristics of critical metal elements in the No. 9 coal from the Xinyuan mine of the northern Qinshui coalfield, Shanxi Province, and evaluate the factors influencing its enrichment with critical metal elements.

2. Geological Setting

The Qinshui coalfield is located between the Taiyue Mountain and the middle southern section of the Taihang Mountain in the southeast of Shanxi Province. The coal-bearing area of the Qinshui coalfield is 32,084 km^2. The main coal-bearing strata are the Carboniferous Taiyuan formation and the Permian Shanxi formation. The Taiyuan formation is mainly composed of limestone and clastic rocks, and has several layers of coal seams. It results from the interactive deposition of the lagoon–tidal flat and the carbonate platform against the background of the epicontinental sea. The Shanxi formation is dominated by clastic rocks, with several layers of coal seams, which are a set of shallow water delta deposits. The Shanxi formation shows characteristics of coastal transgression and regression, and gradually transitions to fluvial facies deposition. The coal rank distribution within the Qinshui Basin was intimately associated with magmatic activity due to a tectono-thermal event during the Yanshanian Orogeny of the Late Jurassic/Early Cretaceous age [20].

The Xinyuan mine is located in Yangquan mining area of the northern Qinshui coalfield and covers an area of 135.66 km^2, with an intended production capacity of 5 million tons per year. The Xinyuan mine is currently mining the No. 3 and the No. 9 coals. The No. 9 coal is located in the middle of the Taiyuan formation. The thickness of the coal seam ranges from 0 m to 5.79 m, with an average thickness of 2.03 m. It is a thin-thick coal seam with a mining index of 0.69 and a thickness variation coefficient of 76%. The floor is mainly composed of mudstone, sandy mudstone, fine sandstone, and siltstone.

3. Sampling and Analytical Techniques

A total of 13 samples were collected from a vertical profile of the No. 9 coal in the working face at the Xinyuan mine, including 10 coal samples and 3 roof samples. From top to bottom, the samples were labeled XY-D1, XY-D2, XY-D3, XY-M1, XY-M2, XY-M3, XY-M4, XY-M5, XY-M6, XY-M7, XY-M8, XY-M9, and XY-M10. The roof sample XY-D1, XY-D2 and XY-D3 was made up of a pyrite layer, carbonaceous mudstone and mudstone, respectively. After sampling, all samples were immediately packed in plastic bags to minimize oxidation and contamination.

Proximate analyses were conducted to determine the moisture content, ash yield and volatile matter yield of the collected samples based on ASTM Standard D7582-2015 [23]. The contents of C, H, and N were determined using an elemental analyzer (Leco CHN628SO, St. Joseph, MI, USA). The total sulfur ($S_{t,d}$) was determined based on the Chinese Standard Method GB/T 214-2007 [24]; the forms of sulfur ($S_{p,d}$, pyritic sulfur; $S_{s,d}$, sulfate sulfur; $S_{o,d}$, organic sulfur) were determined based on the Chinese Standard Method GB/T 215-2003 [25].

The mineral contents and compositions were determined using an X-ray powder diffractometer (XRD, Rigaku, SmartLab, Osaka, Japan). The morphology and modes of occurrence were observed using a field emission scanning electron microscope (FE-SEM, Tescan, Mira3-LMU, Brno, Czech) equipped with an energy-dispersive X-ray spectrometer (EDS, Oxford, MAX-20, High Wycombe, UK).

The concentrations of the major element oxides were measured using an X-ray fluorescence spectrometer (XRF, Regaku, ZSXPrimusIV, Osaka, Japan). The concentrations of trace elements were determined using an inductively coupled plasma mass spectrometer (ICP-MS, ThermoFisher, iCAP Q, Bremen, Germany).

The main steps of the sample digestion were as follows: (30 $\pm$ 0.4) mg samples were weighed and ground to less than 200 mesh and placed into the digestion tank, and 2 mL HNO_3, 0.5 mL HF and 0.25 mL $HClO_4$ were added in turn. The digestion tank was numbered and placed on the electric heating plate for cold digestion. After the gas was completely released, the samples were kept in the oven at 180 °C for 12 h. After cooling, the digestion tank was taken out and placed on the electric heating plate for treatment. When the solution was gelatinized, 2mL diluted nitric acid was added to mix it. Then, the digestion tank was placed in the oven at 165 °C for 5 h, taken out and cooled, and then filled to (30 ± 0.1) g with pure water.

4. Results and Discussion

4.1. Coal Chemistry

Table 1 shows the result of proximate analysis, ultimate analysis, total sulfur, and forms of sulfur from the No. 9 coal and roof samples of the Xinyuan mine. The moisture content in the No. 9 coal ranges from 0.61% to 1.02%, with an average value of 0.82%. The ash yield ranges from 14.81% to 41.00%, with an average of 28.90%. The volatile matter yield ranges from 13.01% to 20.65%, with an average of 16.53%. The total sulfur content ranges from 0.33% to 0.59%, with an average of 0.43%. According to the Chinese Standard GB/T 15224.1-2018 [26] and GB/T 15224.2-2010 [27], coal samples XY-M1~XY-M4 in the No. 9 coal are ultra-low sulfur and medium-high ash coal, coal samples XY-M5~XY-M8 are low-sulfur and low-ash coal, and coal samples XY-M9~XY-M10 are ultra-low sulfur and medium-high ash coal.

Table 1. Proximate and ultimate analysis and sulfur contents of the No. 9 coal and related roof samples from the Xinyuan mine (%).

Sample	M_{ad} [1]	A_d [2]	V_{daf} [3]	C_{daf} [4]	H_{daf} [5]	O_{daf} [6]	N_{daf} [7]	$S_{t,d}$ [8]	$S_{p,d}$ [9]	$S_{s,d}$ [10]	$S_{o,d}$ [11]
XY-D1	0.88	69.41	12.00	nd [12]	nd	nd	nd	7.87	6.65	0.18	1.04
XY-D2	1.06	53.89	11.45	79.40	4.79	7.50	1.58	3.10	2.46	0.20	0.44
XY-D3	0.99	74.23	13.40	nd	nd	nd	nd	0.16	nd	nd	nd
XY-M1	0.70	41.00	13.31	83.91	4.49	9.76	1.28	0.33	0.10	0.02	0.21
XY-M2	0.84	40.86	13.01	83.24	4.61	10.29	1.30	0.33	0.10	0.04	0.19
XY-M3	0.74	36.21	20.06	85.36	4.33	8.48	1.30	0.34	0.13	0.03	0.18
XY-M4	0.61	36.95	20.65	85.21	4.34	8.64	1.28	0.34	0.08	0.01	0.25
XY-M5	0.98	15.35	14.58	90.34	3.89	2.83	1.31	0.54	0.07	0.00	0.47
XY-M6	0.90	14.81	14.37	90.17	3.92	3.79	1.47	0.55	0.06	0.00	0.49
XY-M7	1.02	15.84	14.79	90.28	3.91	3.64	1.51	0.56	0.08	0.00	0.48
XY-M8	1.02	17.15	14.95	89.79	4.00	3.97	1.54	0.59	0.09	0.00	0.50
XY-M9	0.68	34.86	19.60	86.12	4.22	7.74	1.36	0.36	0.07	0.00	0.29
XY-M10	0.68	35.94	19.99	84.78	4.21	9.11	1.35	0.35	0.07	0.00	0.28

[1] M, moisture; ad, air-dry basis; [2] A, ash yield; d, dry basis; [3] V, volatile matter yield; daf, dry and ash-free basis; [4] C, carbon; [5] H, hydrogen; [6] O, oxygen; [7] N, nitrogen; [8] S_t, total sulfur; [9] S_p, pyritic sulfur; [10] S_s, sulfate sulfur; [11] S_o, organic sulfur; [12] no data; [12] nd, no data.

4.2. Mineral Compositions

The mineral compositions of the No. 9 coal and related roof samples from the Xinyuan mine are shown in Table 2. The major minerals (>3%) in the roof samples are primarily represented by clay minerals and quartz, and to a lesser extent, by pyrite and ankerite. Scanning electron microscope (SEM) images of the roof sample XY-D1 (pyrite layer) show that most of the pyrites are broken (Figure 1A) and scattered in clay minerals and organic matter (Figure 1B).

The major minerals (>3%) in the upper part of the No. 9 coal (samples XY-M1~XY-M4) are clay minerals and quartz, followed by the minor minerals (>1%) such as anatase, magnesite, gypsum, barite, etc. SEM images of the sample XY-M1 show that the clay minerals mainly occur in the infillings of cell cavities, or are mixed with the organic matter (Figure 1C); the anatases are embedded in organic matter as blocks or layers (Figure 1D). The major minerals in the middle part of the No. 9 coal (samples XY-M5~XY-M8) are clay minerals, quartz, calcite, dolomite, ankerite, analcime, barite and anatase, and the mineral compositions are mainly characterized by a higher content of carbonate minerals. SEM images of the sample XY-M7 show that carbonate minerals coexist closely with clay minerals (Figure 1E) and organic matter (Figure 1F). The mineral compositions of the lower part of the No. 9 coal (sample XY-M9~XY-M10) are similar to the upper part; the major minerals are clay minerals, quartz and anatase with occasional siderite, gypsum, etc.

Table 2. Mineral compositions of the No. 9 coal and related roof samples from the Xinyuan mine, determined by XRD (%).

Sample	Qz [1]	CM [2]	Cal [3]	Dlm [4]	Ank [5]	Py [6]	Sd [7]	Mag [8]	Gp [9]	Fsp [10]	Anc [11]	Bar [12]	Ant [13]
XY-D1	37.8 *	47.7 *	- [14]	-	-	10.1 *	-	-	-	0.5	1.0	1.1	1.8
XY-D2	23.5 *	65.7 *	-	-	3.9 *	2.8	-	-	-	0.4	-	1.7	2.0
XY-D3	25.2 *	72.4 *	-	-	-	-	-	-	0.3	-	-	-	2.1
XY-M1	12.7 *	82.6 *	-	-	-	-	-	2.1	-	-	-	-	2.6
XY-M2	11.7 *	79.7 *	-	-	-	-	-	1.7	2.0	-	2.3	2.6	-
XY-M3	12.0 *	80.0 *	-	-	-	-	1.0	2.0	2.0	-	3.0	-	-
XY-M4	12.5 *	82.6 *	-	-	-	-	-	2.0	2.9	-	-	-	-
XY-M5	6.9 *	59.1 *	5.9 *	5.5 *	5.5 *	-	1.4	0.9	-	0.9	6.5 *	7.4 *	-
XY-M6	7.7 *	62.6 *	4.0 *	-	0.9	-	2.3	0.6	-	1.5	6.9 *	7.7 *	5.8 *
XY-M7	7.0 *	71.6 *	4.2 *	4.8 *	-	-	2.0	2.5	-	1.7	-	-	6.2 *
XY-M8	14.5 *	77.3 *	0.6	-	-	-	1.9		-	-	-	-	5.7 *
XY-M9	12.0 *	80.2 *	-	-	-	-	1.6	2.1	-	0.6	-	-	3.5 *
XY-M10	12.9 *	80.0 *	-	-	-	-	-	2.8	1.7	-	-	-	2.6

[1] Qz, quartz; [2] CM, clay minerals; [3] Cal, calcite; [4] Dlm, dolomite; [5] Ank, ankerite; [6] Py, pyrite; [7] Sd, siderite; [8] Mag, magnesite; [9] Gp, gypsum; [10] Fsp, feldspar; [11] Anc, analcime; [12] Bar, Barite; [13] Ant, anatase; -, not identified or below detection of XRD; *, major mineral (>3%).

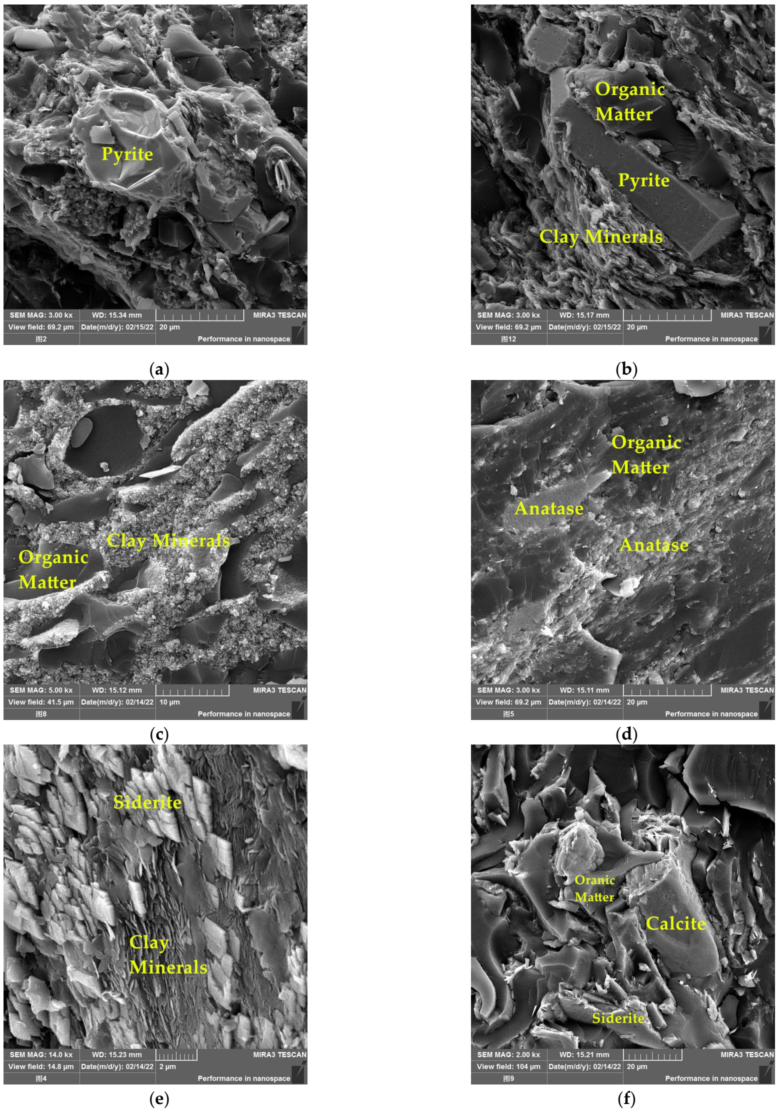

Figure 1. SEM images of minerals in the No. 9 coal and related roof samples from the Xinyuan mine: (**a**) Pyrite in sample XY-D1; (**b**) Pyrite and clay minerals in sample XY-D1; (**c**) Clay minerals in sample XY-M1; (**d**) Anatase in sample XY-M1; (**e**) Siderite and clay minerals in sample XY-M7; (**f**) Siderite and calcite in sample XY-M7.

4.3. Concentrations of Major and Minor Element Oxides

The studied elements can be grouped as major elements (>1%), minor elements (1–0.1%) and trace elements (<0.1%). The concentrations of major and minor elements are shown as oxides and listed in Table 3. The major element oxides in the No. 9 coal are dominated by SiO_2 and Al_2O_3. The concentration of SiO_2 ranges from 14.81% to 41.00%, with an average of 13.89%; the concentration of Al_2O_3 content ranges from 5.73% to 18.36%, with an average of 12.48%. Compared with the average value of major and minor element oxides in common Chinese coal [28], the No. 9 coal from the Xinyuan mine has relatively higher concentrations of SiO_2, Al_2O_3 and TiO_2, and lower concentrations of Fe_2O_3, CaO, MgO, P_2O_5, Na_2O, K_2O. Vertically, the upper and lower part of the No. 9 coal from the Xinyuan mine (sample XY-M1~XY-M4, XY-M9~XY-M10) are mainly characterized by higher SiO_2, Al_2O_3, TiO_2 and lower CaO, while the middle part of the No. 9 coal (sample XY-M5~XY-M8) is mainly characterized by higher CaO and lower SiO_2, Al_2O_3, and TiO_2. The vertical distribution of the major and minor element oxides (Table 3) is coherent with the mineral compositions (Table 2).

Table 3. Concentrations of major and minor element oxides (%) in the No. 9 coal and related roof samples (on whole coal/rock basis) from the Xinyuan mine.

Sample	SiO_2	Al_2O_3	Fe_2O_3	CaO	MgO	TiO_2	P_2O_5	K_2O	Na_2O
XY-D1	36.68	19.16	11.10	0.11	0.17	1.24	0.03	0.57	0.36
XY-D2	29.84	16.39	4.21	0.26	0.23	0.73	0.05	0.77	0.26
XY-D3	37.87	32.01	1.20	0.12	0.15	0.86	0.05	0.51	0.21
XY-M1	20.27	18.25	0.76	0.30	0.10	0.53	0.04	0.07	0.11
XY-M2	20.36	18.36	0.68	0.20	0.07	0.55	0.04	0.07	0.13
XY-M3	17.89	16.13	0.68	0.18	0.07	0.49	0.04	0.06	0.10
XY-M4	18.31	16.47	0.56	0.19	0.06	0.77	0.06	0.06	0.10
XY-M5	6.86	6.02	0.77	0.62	0.09	0.14	0.02	0.02	0.14
XY-M6	6.62	5.73	1.10	0.33	0.11	0.16	0.01	0.02	0.15
XY-M7	7.08	6.15	0.93	0.45	0.10	0.22	0.03	0.03	0.14
XY-M8	7.75	6.65	0.89	0.53	0.10	0.23	0.10	0.04	0.12
XY-M9	16.29	14.99	1.40	0.22	0.16	0.68	0.16	0.06	0.13
XY-M10	17.44	15.99	0.71	0.13	0.09	0.52	0.10	0.05	0.12
AV-C [1]	13.89	12.48	0.85	0.31	0.10	0.43	0.06	0.05	0.12
AV-R [2]	34.80	22.52	5.50	0.16	0.18	0.94	0.05	0.62	0.28
Chinese coal [3]	8.47	5.98	4.85	1.23	0.22	0.33	0.092	0.19	0.16

[1] AV-C, average concentration in coal samples; [2] AV-R, average concentration in roof samples; [3] Chinese coal; average values in Chinese coal from Dai et al. [28].

The average ratio of SiO_2/Al_2O_3 is 1.12, which is higher than the average of Chinese coal (1.42), indicating a higher level of Al_2O_3. Coal with $Al_2O_3 \geq 40\%$ in ash is called high-aluminum coal; the concentration of Al_2O_3 in ashes from the No. 9 coal of the Xinyuan mine ranges from 38.72% to 44.94%, with an average of 42.16%, reaching the standard of high-aluminum coal. The fly ash produced by the combustion of high-aluminum coal can be used as a substitute for bauxite to prepare alumina, which has high exploitation and utilization potential.

4.4. Concentrations of Trace Elements

The concentrations of trace elements in the No. 9 coal and roof samples from the Xinyuan mine are shown in Table 4. Figure 2 shows the concentration coefficients (CC [29], the ratio of elemental concentrations between the studied sample and world hard coal). Compared with world hard coals [30], the No. 9 coal from the Xinyuan mine is enriched (CC > 5) with Li (CC = 8.00) and Th (CC = 5.41), slightly enriched (2 < CC < 5) with Pb (CC = 4.84), Sc (CC = 2.24), Ga (CC = 3.48), Y (CC = 2.74), La (CC = 2.09), Ce (CC = 2.42), Tb (CC = 2.29), Dy (CC = 2.02), Er (CC = 2.50), Yb (CC = 2.31) and Hg (CC = 2.71), and depleted(CC < 0.5) in Mn, Co, Ni, Rb, Cs and Tl; the rest of the trace elements have similar concentration levels to the average of world hard coal.

Table 4. Concentrations of trace elements (μg/g) in the No. 9 coal and related roof samples from the Xinyuan mine.

Sample	XY-D1	XY-D2	XY-D3	XY-M1	XY-M2	XY-M3	XY-M4	XY-M5	XY-M6	XY-M7	XY-M8	XY-M9	XY-M10	AV-C [1]	AV-R [2]	Chinese Coal [3]	World Coal [4]	World Clay [5]	CC [6]
Li	120	48.2	89.8	144	142	144	140	53.6	46.4	45.8	47.6	165	191	111.9	86.0	31.8	14	54	8.00
Sc	12.1	10.9	7.7	12.2	10.2	10.8	16.2	3.55	3.88	3.37	3.70	9.36	9.58	8.28	10.2	4.38	3.7	15	2.24
V	63	63	69	18	19	20	27	17	17	20	19	26	22	20.50	65.0	35.1	28	120	0.73
Cr	50.0	38.2	22.0	15.2	14.5	14.5	24.0	8.92	9.31	9.48	11.3	16.8	18.0	14.20	36.7	15.4	17	110	0.84
Mn	44.9	82.2	27.4	32.2	18.9	20.1	17.1	32.6	25.3	30.7	33.3	22.6	13.3	24.61	51.5	94.8	71		0.35
Co	12.8	8.99	6.62	1.12	2.09	0.95	0.89	1.64	1.88	1.92	2.10	0.850	0.496	1.39	9.47	7.08	6.0	19	0.23
Ni	86.2	16.9	12.9	5.82	6.06	5.00	6.22	2.79	2.94	2.98	3.74	2.72	4.15	4.24	38.7	13.7	17	49	0.25
Cu	33.1	32.6	18.0	26.4	25.8	23.9	39.0	15.5	28.8	22.0	22.4	31.6	34.4	26.98	27.9	17.5	16	36	1.69
Zn	31.4	45.8	71.9	24.3	25.4	24.6	38.4	8.67	7.26	6.16	7.20	13.4	8.57	16.40	49.7	41.4	28	89	0.59
Ga	32	39	31	22	27	21	20	18	20	18	20	24	19	20.9	34.0	6.55	6.0	16	3.48
Ge	8	8	5	3	3	3	3	2	2	2	3	3	3	2.7	7.0	2.78	2.4	2	1.13
Rb	40.0	69.9	33.2	4.55	4.16	3.01	3.53	1.20	0.950	1.07	2.16	2.12	1.94	2.47	47.7	9.25	18	133	0.14
Sr	108	144	137	124	152	129	160	136	73	92	129	642	335	197	130	140	100	240	1.97
Y	18.7	35.5	21.5	33.0	27.1	31.3	42.0	13.2	10.6	10.4	12.8	19.3	24.8	22.45	25.2	18.2	8.2	31	2.74
Mo	16.6	8.14	2.72	1.68	2.82	1.92	3.44	2.66	2.82	2.96	3.35	3.05	2.11	2.68	9.15	3.08	2.1	1.6	1.28
Cs	4.41	9.05	3.16	0.422	0.437	0.318	0.358	0.135	0.122	0.163	0.311	0.232	0.222	0.27	5.54	1.13	1.1	13	0.25
Ba	232	252	248	102	125	124	119	73	60	68	78	184	140	107	244	159	150	460	0.72
La	36.8	63.4	49.3	17.0	16.2	15.6	20.8	14.2	14.6	16.2	22.4	58.5	34.6	23.01	49.83	22.5	11	48	2.09
Ce	84.0	138	104	55.9	52.7	57.8	67.3	30.1	30.4	32.7	43.2	104	83.6	55.77	108.67	46.7	23	75	2.42
Pr	7.08	13.0	10.4	6.40	5.55	6.26	8.18	3.29	3.18	3.41	4.40	8.08	7.88	5.66	10.16	6.42	3.4	10	1.67
Nd	24.4	48.3	36.2	25.2	21.5	24.5	31.6	12.0	11.2	12.0	15.6	23.8	27.7	20.51	36.30	22.3	12	36	1.71
Sm	4.35	8.04	5.65	5.66	4.66	5.26	7.12	2.38	2.05	2.14	2.76	3.61	5.08	4.07	6.01	4.07	2.2	8	1.85
Eu	0.754	1.47	1.02	1.14	0.988	1.02	1.46	0.510	0.403	0.408	0.524	0.750	0.866	0.81	1.08	0.84	0.43	1.2	1.88
Gd	4.52	8.00	5.96	5.59	4.90	5.19	6.95	2.53	2.12	2.19	2.88	4.36	5.23	4.19	6.16	4.65	2.7	5.8	1.55
Tb	0.719	1.12	0.914	0.980	0.859	0.924	1.24	0.447	0.348	0.344	0.435	0.646	0.864	0.71	0.92	0.62	0.31	0.83	2.29
Dy	4.22	6.48	5.23	5.98	5.10	5.68	7.66	2.50	2.04	1.98	2.48	3.82	5.14	4.24	5.31	3.74	2.1	4.4	2.02
Ho	0.797	1.36	0.994	1.19	0.986	1.13	1.51	0.504	0.414	0.392	0.488	0.757	0.988	0.84	1.05	0.96	0.57	0.9	1.47
Er	2.37	4.41	2.94	3.58	2.90	3.38	4.52	1.43	1.26	1.19	1.46	2.32	2.94	2.50	3.24	1.79	1.00	1.9	2.50
Tm	0.332	0.645	0.398	0.494	0.398	0.468	0.621	0.220	0.184	0.169	0.204	0.330	0.404	0.35	0.46	0.64	0.30	0.5	1.16
Yb	2.26	4.62	2.69	3.28	2.65	3.10	4.10	1.30	1.20	1.14	1.38	2.26	2.70	2.31	3.19	2.08	1.0	2.5	2.31
Lu	0.331	0.708	0.384	0.458	0.371	0.433	0.573	0.203	0.178	0.164	0.201	0.320	0.374	0.33	0.47	0.38	0.20	0.39	1.64
Hg		0.365		0.250	0.296	0.305	0.342	0.274	0.196	0.230	0.305	0.263	0.247	0.27		0.163	0.10	0.068	2.71

Table 4. *Cont.*

Sample	XY-D1	XY-D2	XY-D3	XY-M1	XY-M2	XY-M3	XY-M4	XY-M5	XY-M6	XY-M7	XY-M8	XY-M9	XY-M10	AV-C [1]	AV-R [2]	Chinese Coal [3]	World Coal [4]	World Clay [5]	CC [6]
Tl	1.80	1.64	0.538	0.089	0.084	0.098	0.072	0.069	0.052	0.061	0.082	0.066	0.060	0.07	1.33	0.47	0.58	1.3	0.13
Pb	284	34.8	56.3	64.3	45.2	49.6	111	14.3	24.6	20.8	24.6	40.4	41.2	43.6	125.0	15.1	9.0	14	4.84
Th	34	15	20	20	22	17	35	7	7	8	8	30	19	17.3	23.0	5.84	3.2	14	5.41
U	9	5	5	4	7	5	7	2	2	2	2	5	5	4.1	6.3	2.43	1.9	4.3	2.16
∑REY [7]	191.6	335.1	247.6	165.9	146.9	162.0	205.6	84.8	80.2	84.8	111.2	232.9	203.2	147.74	258.09	135.89	68.41	226.4	2.16

[1] AV-C, average concentration of coal samples; [2] AV-R, average concentration of roof samples; [3] Chinese coal, average values in Chinese coal from Dai et al. [28]; [4] World coal, average values in hard coal from around the world from Ketris and Yudovich [30]; [5] World clay, average values in clay from around the world from Grigoriev [31]; [6] CC, concentration coefficient = AV-C/World coal; [7] ∑REY, total rare earth elements and yttrium.

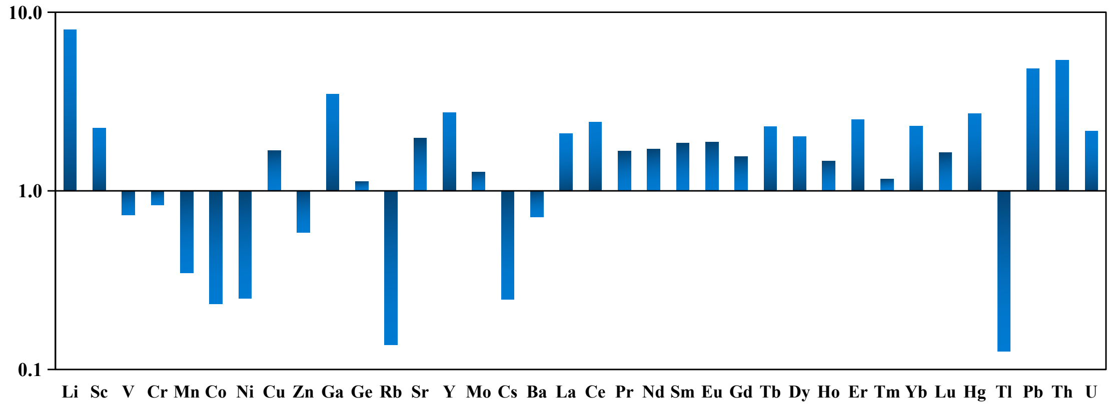

Figure 2. Concentration coefficients of trace elements in the No. 9 coal and related roof samples from the Xinyuan mine.

4.5. Geochemical Characteristics of Selected Critical Metal Elements

4.5.1. Li

The distribution area of lithium-rich coal in China is mainly located in the Junger coalfield of Inner Mongolia [32], the Ningwu coalfield [33–35] and the Jincheng mining area of Shanxi [20]. The concentrations of Li in the No. 9 coal from the Xinyuan mine range from 45.8 to 191 µg/g, with an average value of 111.9 µg/g, which is much higher than the average value of world coal [30] and Chinese coal [28]. According to the concentration coefficient (CC) classification levels proposed by Dai et al. [29], the CC value of Li in the No. 9 coal from the Xinyuan mine is 8.00, which is classified as an enrichment level of (5 < CC < 10), close to a high enrichment level (CC > 10). The vertical distribution of Li in the No. 9 coal is shown in Figure 3. The concentrations of Li in the roofs range from 48.2 to 120 µg/g, with an average value of 86.0 µg/g. The concentrations of Li in the upper part of the No. 9 coal (sample XY-M1~XY-M4) are higher, with an average value of 142.5 µg/g; the concentrations of Li in the middle part of the No. 9 coal (sample XY-M5~XY-M8) are lower, with an average value of 48.35 µg/g; the concentrations of Li in the lower part of the No. 9 coal (sample XY-M9~XY-M10) are the highest, with an average value of 178 µg/g.

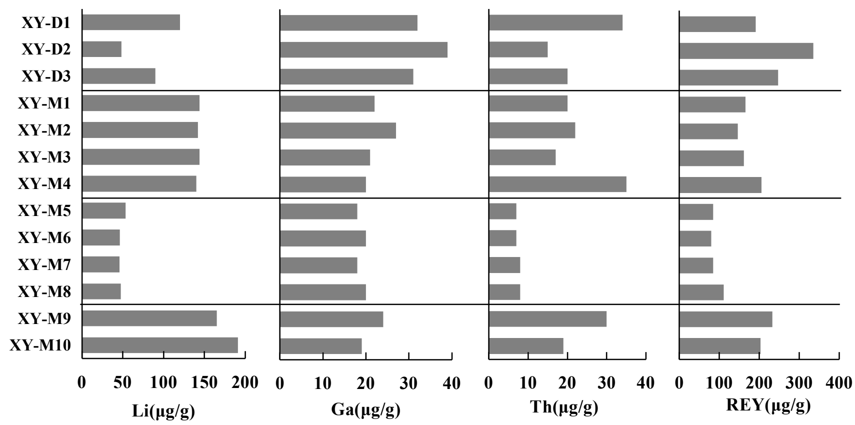

Figure 3. Vertical distribution of Li, Ga, Th and REY in the No. 9 coal and related roof samples from the Xinyuan mine.

4.5.2. Ga

The distribution area of gallium-rich coal in China is mainly located in Junger coalfield [36,37] and the Daqingshan coalfield [38,39] in Inner Mongolia. The concentrations of Ga in the No. 9 coal from the Xinyuan mine range from 18 to 27 µg/g, with an average value of 20.9 µg/g, which is higher than the average value of world coal and Chinese coal. According to the concentration coefficient (CC) classification levels proposed by Dai et al. [29], the CC value of Ga in the No. 9 coal from the Xinyuan mine is 3.48, which is classified as slightly enriched. The vertical distribution of Ga in the No. 9 coal is shown in Figure 3. The concentrations of Ga in the roofs range from 31 μg/g to 39 μg/g, with an average value of 34 μg/g. The average concentration of Ga in the upper part of the No. 9 coal (sample XY-M1~XY-M4) is 22.5 μg/g, and the average concentration of Ga in the middle part of the No. 9 coal (sample XY-M5~XY-M8) is 19 μg/g; the average concentration of Ga in the lower part of the No. 9 coal (sample XY-M9~XY-M10) is 21.5 μg/g. Vertically, there is little difference in the concentrations of Ga in the No. 9 coal.

4.5.3. Th

The concentrations of Th in the No. 9 coal from the Xinyuan mine range from 7 μg/g to 35 μg/g, with an average value of 17.3 μg/g, which is higher than that in world coal and Chinese coal. According to the concentration coefficient (CC) classification levels proposed by Dai et al. [29], the CC value of Th in the No. 9 coal from the Xinyuan mine is 5.41, which is classified as slightly enriched. The vertical distribution of Th is shown in Figure 3. The vertical distribution of Th is similar to Li. The concentrations of Th in the roofs range from 15 μg/g to 34 μg/g, with an average value of 23 μg/g. The concentrations of Th in the upper part of the No. 9 coal (sample XY-M1~XY-M4) are higher, with an average value of 23.5 μg/g; the concentrations of Th in the middle part of the No. 9 coal (sample XY-M5~XY-M8) are lower, with an average value of 7.5 μg/g; and the concentrations of Th in the lower part of the No. 9 coal (sample XY-M9~XY-M10) are the highest, with an average value of 24.5 μg/g.

4.5.4. Modes of Occurrence of Li, Ga and Th

Previous studies have shown that Li in coal mainly occurs in silicate minerals [40], especially in clay minerals and muscovite [41]; Ga in coal mainly occurs in clay minerals [40], partly in boehmite or diaspore [36,37,42], and Th in coal mainly occurs in aluminosilicate minerals [40]. The Pearson correlation coefficients between Li, Ga, Th, REY, ash yield, total sulfur and some major oxides in the No. 9 coal from the Xinyuan mine are shown in Table 5. Li, Ga and Th have substantial positive correlations with ash yield, with correlation coefficients of 0.924, 0.640 and 0.810, respectively, indicating that Li, Ga and Th mainly exist in inorganic components. Li, Ga and Th are negatively correlated with total sulfur, indicating that they do not occur in sulfur minerals. The correlation coefficients of Li, Ga and Th with SiO_2 are 0.912, 0.633 and 0.799, respectively, and the correlation coefficients of Li, Ga and Th with Al_2O_3 are 0.922, 0.632 and 0.804, respectively, indicating that Li, Ga and Th mainly occur in aluminum silicates. Clay minerals may be the main carrier.

Table 5. Correlations between Li, Ga, Th, REY, ash yield, total sulfur and some major oxides in the No. 9 coal and related roof samples from the Xinyuan mine.

	A_d	$S_{t,d}$	SiO_2	Al_2O_3	Li	Ga	Th	REY
Li	0.924 **	−0.943 **	0.912 **	0.922 **	-	-	-	-
Ga	0.640 *	−0.578	0.633 *	0.632	0.480	-	-	-
Th	0.810 **	−0.834 **	0.799 **	0.804 **	0.789 **	0.502	-	-
REY	0.822 **	−0.824 **	0.801 **	0.813 **	0.917 **	0.413	0.902 **	-

**, The correlation is significant at the 0.01 level (double tailed); *, The correlation is significant at the 0.05 level (double tailed).

4.6. Geochemical Characteristics of Rare Earth Elements

The concentrations of REY in the No. 9 coal from the Xinyuan mine range from 80.18 μg/g to 232.85 μg/g, with an average value of 147.74 μg/g (Table 6), which is higher than that in world coal and Chinese coal. The concentrations of REY in the roofs range from 191.63 μg/g to 335.05 μg/g (Figure 3), with an average value of 258.09 μg/g, which is higher than the average concentration of REY in coal. The upper part of the No. 9 coal (samples XY-M1~XY-M4) has higher concentrations of REY, with an average value of 170.10 μg/g, while the middle part of the No. 9 coal (samples XY-M5~XY-M8) has lower concentrations of REY, with an average value of 90.26 μg/g; the lower part of the No. 9 coal (samples XY-M9~XY-M10) has the highest concentration level of REY, with an average of 218.01 μg/g. The vertical distribution of REY is consistent with the ash yield, SiO_2, Al_2O_3, Li and Th. The correlation coefficients of REY with ash yield, Al_2O_3 and SiO_2 are 0.822, 0.801 and 0.813, respectively, suggesting that REY mainly occurs in aluminosilicate minerals.

REY is classified into three categories, following Seredin and Dai [43]: LREY (Light REY), including La, Ce, Pr, Nd and Sm; MREY (Medium REY), including Eu, Gd, Tb, Dy and Y; and HREY (heavy REY), including Ho, Er, Tm, Yb and Lu. The corresponding enrichment types of REY are also classified into L-type ($La_N/Lu_N > 1$), M-type ($La_N/Sm_N < 1$ and $Gd_N/Lu_N > 1$) and H-type ($La_N/Lu_N < 1$) (Table 6). The concentrations of rare earth elements in the No. 9 coal are normalized to the average concentrations of the upper continental crust (UCC) [44]. The distribution patterns of REY in the No. 9 coal and related roof samples from the Xinyuan mine are shown in Figure 4.

Table 6. Geochemical parameters of REY in the No. 9 coal and related roof samples from the Xinyuan mine.

Sample	ΣLREY [1]	ΣMREY [2]	ΣHREY [3]	ΣREY [4]	La_N/Lu_N [5]	La_N/Sm_N	Gd_N/Lu_N	Ce_N/Ce_N^* [6]	Eu_N/Eu_N^* [7]	Type
XY-D1	156.63	28.91	6.09	191.63	1.19	1.27	1.15	1.18	0.79	L [8]
XY-D2	270.74	52.57	11.74	335.05	0.96	1.18	0.95	1.09	0.86	H [9]
XY-D3	205.55	34.62	7.41	247.58	1.37	1.31	1.31	1.05	0.82	L
XY-M1	110.16	46.69	9.00	165.85	0.40	0.45	1.03	1.19	0.95	M [10]
XY-M2	100.61	38.95	7.31	146.86	0.47	0.52	1.11	1.25	0.97	M
XY-M3	109.42	44.11	8.51	162.05	0.38	0.44	1.01	1.29	0.91	M
XY-M4	135.00	59.31	11.32	205.63	0.39	0.44	1.02	1.14	0.97	M
XY-M5	61.97	19.19	3.66	84.81	0.75	0.89	1.05	1.00	0.97	M
XY-M6	61.43	15.51	3.24	80.18	0.87	1.07	1.00	1.02	0.90	H
XY-M7	66.45	15.32	3.06	84.83	1.05	1.14	1.12	1.00	0.88	L
XY-M8	88.36	19.12	3.73	111.21	1.19	1.22	1.21	0.99	0.87	L
XY-M9	197.99	28.88	5.99	232.85	1.95	2.43	1.15	1.05	0.87	L
XY-M10	158.86	36.90	7.41	203.17	0.99	1.02	1.18	1.15	0.79	H

[1] ΣLREY, total concentration of light REY elements (La, Ce, Pr, Nd and Sm); [2] ΣMREY, total concentration of medium REY elements (Eu, Gd, Tb, Dy and Y); [3] ΣHREY, total concentration of heavy REY elements (Ho, Er, Tm, Yb and Lu); [4] ΣREY, total concentration of rare earth elements and yttrium; [5] N, values normalized by the average concentration of REY in the upper continental crust [44]; [6] $Ce_N/Ce_N^* = 2 \times Ce_N/(La_N + Pr_N)$; [7] $Eu_N/Eu_N^* = 2 \times Eu_N/(Sm_N + Gd_N)$; [8] L, L-type, LaN/LuN > 1; [9] H, H-type, LaN/LuN < 1; [10] M, M-type, LaN/SmN < 1 and GdN/LuN > 1.

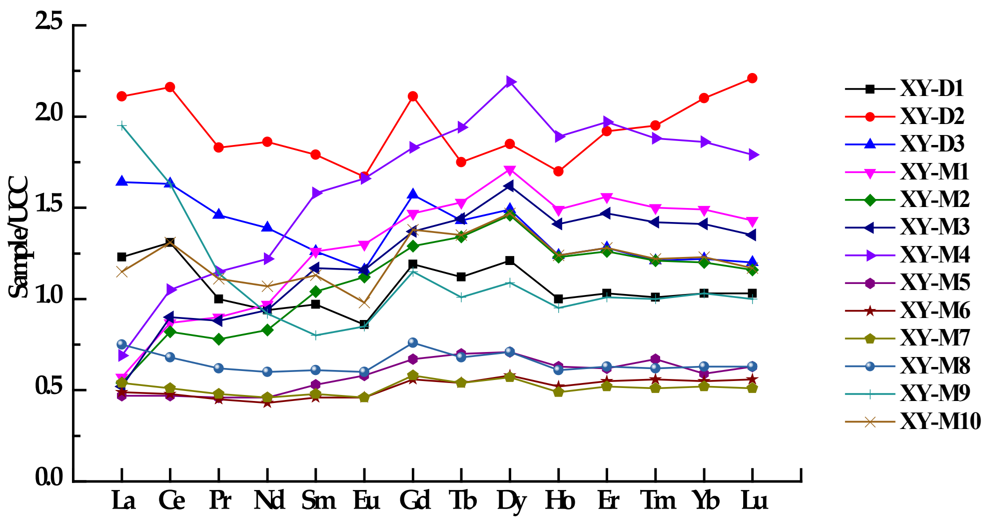

Figure 4. Distribution patterns of REY in the No. 9 coal and related roof samples from the Xinyuan mine; values are normalized by the average concentration of REY in upper continental crust [44].

The REY enrichment type in the upper part of the No. 9 coal from the Xinyuan mine is M-type, while in the middle and lower part of the No. 9 coal, the REY enrichment types are

L-type and H-type. The REY enrichment types in the roof samples are L-type and H-type. The Eu_N/Eu_N^* values of the No. 9 coal range from 0.79 to 0.97, with an average of 0.91, showing slight negative Eu anomalies. Most of the negative Eu anomalies are inherited from the source rocks [45], indicating that the main source of REY is terrigenous debris. The average Eu_N/Eu_N^* value of the roof samples is 0.82, suggesting a greater influence of terrigenous debris. The Ce_N/Ce_N^* values of the No. 9 coal range from 0.99 to 1.29, with an average value of 1.11. Generally, there are no significant Ce anomalies in the No. 9 coal, while the Ce_N/Ce_N^* values in the middle and lower part of the No. 9 coal are lower than that in the upper part. The negative Ce anomalies indicate that the lower part of the No. 9 coal is more affected by the seawater [46].

4.7. Enrichment Mechanism of Critical Metal Elements in Coal

The genetic types of trace element enrichment in Chinese coals mainly include source rock-controlled, marine environment-controlled, hydrothermal fluid-controlled, groundwater-controlled, and volcanic ash-controlled types. [28]. The concentrations of critical metal elements such as Li, Ga, Th and REY in the No. 9 coal from the Xinyuan mine are distributed in a pattern of high in the upper part, low in the middle part and high in the lower part, which is consistent with the distribution of ash yield, SiO_2 and Al_2O_3; thus, the Li, Ga, Th and REY mainly occur in aluminosilicate minerals, i.e., clay minerals. SEM images show that the clay minerals, calcite, siderite and organic matter in the No. 9 coal and roof samples are mixed with each other, and some of the mineral crystals had been broken into fragments, which may suggest a transporting process. The genetic type of critical metal elements such as Li, Ga, Th and REY in the No. 9 coal from the Xinyuan mine is source rock-controlled type.

The critical metal minerals and solutions from the source area were transported to the study area by the action of water. Due to a change in swamp water conditions, the critical metal elements were combined with clay minerals and enriched the coal. The No. 9 coal from the Xinyuan mine can be divided into upper, middle and lower parts according to the vertical distribution of the critical metal elements. The upper and lower parts of the No. 9 coal have a higher concentration of critical metal elements due to a higher content of clay minerals. The clay minerals are negatively charged in nature and have a high surface-to-volume ratio, which enables the critical metal elements, usually positively charged, to be adsorbed [47]. However, the higher content of carbonate minerals in the middle part of the No. 9 coal leads to the weakening of its adsorption capacity for critical metal elements.

5. Conclusions

The mineral compositions of the No. 9 coal from the Xinyuan mine are primarily represented by clay minerals and quartz, and to a lesser extent, contain a small amount of calcite, siderite, magnesite, anatase, and gypsum. SEM images show that the clay minerals, calcite, siderite and organic matter in the No. 9 coal and roof samples are mixed with each other, and most of the mineral crystals had been broken into fragments, suggesting a transporting process.

The major element oxides in the No. 9 coal are dominated by SiO_2 and Al_2O_3. Compared with the average value of major element oxides in common Chinese coal, the No. 9 coal has relatively higher concentrations of SiO_2, Al_2O_3 and TiO_2, and lower concentrations of Fe_2O_3, CaO, MgO, P_2O_5, Na_2O, and K_2O. The No. 9 coal of the Xinyuan mine is enriched with Li and Th, slightly enriched with Pb, Sc, Ga, Y, La, Ce, Tb, Dy, Er, Yb and Hg, and depleted in Mn, Co, Ni, Rb, Cs and Tl compared with world hard coals. The rest of the trace elements have similar concentration levels to the averages of world hard coal.

The critical metal elements such as Li, Ga, Th and REY that enriched the No. 9 coal mainly occur in aluminum silicates; clay minerals may be the main carrier. The genetic type of the critical metal elements such as Li, Ga, Th and REY in the No. 9 coal from the Xinyuan mine is source rock-controlled type. The critical metal minerals and solutions from the source area were transported to the study area by the action of water. Due to a change in swamp water conditions, the critical metal elements were combined with clay minerals and enriched the coal.

Author Contributions: Conceptualization, J.L.; methodology, J.L.; software, J.L.; validation, S.Z., H.W. and X.X.; formal analysis, J.L.; investigation, J.L.; resources, S.Z., H.W. and X.X.; data curation, J.L.; writing—original draft preparation, J.L.; writing—review and editing, J.L.; visualization, J.L.; supervision, S.Z. and H.W.; project administration, S.Z., H.W. and X.X.; funding acquisition, S.Z., H.W. and X.X. All authors have read and agreed to the published version of the manuscript.

Funding: This research was funded by the National Key Research & Development Program of China (grant number: 2021YFC2902004), the Central Guidance on Local Science and Technology Development Fund Project of Shanxi Province (grant number: YDZX20201400001051) and the National Natural Science Foundation of China (grant number: 41802193, 41902180).

Data Availability Statement: Not applicable.

Acknowledgments: The authors would like to thank the anonymous reviewers for their helpful suggestions and comments.

Conflicts of Interest: The authors declare no conflict of interest.

References

1. Zhang, S.Q.; Zhao, F.H.; Liu, D.N.; Zhao, L.; Zhang, X.H.; Lin, J.W.; Dong, H.Y.; Zhao, S.; Liu, X.F.; Zan, M.J. Modes of Occurrence of Critical Metal Elements (Li, REEs and Other Critical Elements) in Low-Grade Bauxite from Southern Shanxi Province, China. *Minerals* **2022**, *12*, 990. [CrossRef]
2. Dai, S.; Arbuzov, S.I.; Chekryzhov, I.Y.; French, D.; Feole, I.; Folkedahl, B.C.; Graham, I.T.; Hower, J.C.; Nechaev, V.P.; Wagner, N.J.; et al. Metalliferous Coals of Cretaceous Age: A Review. *Minerals* **2022**, *12*, 1154. [CrossRef]
3. Seredin, V.V.; Finkelman, R.B. Metalliferous coals: A review of the main genetic and geochemical types. *Int. J. Coal Geol.* **2008**, *76*, 253–289. [CrossRef]
4. Seredin, V.V.; Dai, S.F.; Sun, Y.Z.; Chekryzhov, I.Y. Coal deposits as promising sources of rare metals for alternative power and energy-efficient technologies. *Appl. Geochem.* **2013**, *31*, 1–11. [CrossRef]
5. Dai, S.F.; Finkelman, R.B. Coal as a promising source of critical elements: Progress and future prospects. *Int. J. Coal Geol.* **2018**, *186*, 155–164. [CrossRef]
6. Dai, S.F.; Yan, X.Y.; Ward, C.R.; Hower, J.C.; Zhao, L.; Wang, X.B.; Zhao, L.X.; Ren, D.Y.; Finkelman, R.B. Valuable elements in Chinese coals: A review. *Int. Geol. Rev.* **2018**, *60*, 590–620. [CrossRef]
7. Hower, J.C.; Granite, E.J.; Mayfield, D.B.; Lewis, A.S.; Finkelman, R.B. Notes on Contributions to the Science of Rare Earth Element Enrichment in Coal and Coal Combustion Byproducts. *Minerals* **2016**, *6*, 32. [CrossRef]
8. Hower, J.C.; Eble, C.F.; Wang, N.; Dai, S.F. Distribution of rare earth elements and other critical elements in beneficiated Pennsylvania anthracites. *Fuel* **2021**, *304*, 121400. [CrossRef]
9. Blissett, R.S.; Smalley, N.; Rowson, N.A. An investigation into six coal fly ashes from the United Kingdom and Poland to evaluate rare earth element content. *Fuel* **2014**, *119*, 236–239. [CrossRef]
10. Fiket, Z.; Medunic, G.; Turk, M.F.; Kniewald, G. Rare earth elements in superhigh-organic-sulfur Rasa coal ash (Croatia). *Int. J. Coal Geol.* **2018**, *194*, 1–10. [CrossRef]
11. Krzeszowska, E.; Kokowska-Pawlowska, M.; Krzeszowski, S. Distribution of Selected Critical Elements in the Carboniferous Coal-bearing Series of the Upper Silesian and Lublin Coal Basins (Poland). *Acta Geol. Sin-Engl.* **2022**, *96*, 273–292. [CrossRef]
12. Nechaev, V.P.; Chekryzhov, I.Y.; Vysotskiy, S.V.; Ignatiev, A.V.; Velivetskaya, T.A.; Tarasenko, I.A.; Agoshkov, A.I. Isotopic signatures of REY mineralization associated with lignite basins in South Primorye, Russian Far East. *Ore Geol. Rev.* **2018**, *103*, 68–77. [CrossRef]
13. Seredin, V.V.; Arbuzov, S.I.; Alekseev, V.P. Sc-bearing coals from Yakhlinsk deposit, Western Siberia. *Dokl. Earth Sci.* **2006**, *409*, 967–972. [CrossRef]
14. Wagner, N.J.; Matiane, A. Rare earth elements in select Main Karoo Basin (South Africa) coal and coal ash samples. *Int. J. Coal Geol.* **2018**, *196*, 82–92. [CrossRef]
15. Di, S.B.; Dai, S.F.; Nechaev, V.P.; Zhang, S.W.; French, D.; Graham, I.T.; Spiro, B.; Finkelman, R.B.; Hou, Y.J.; Wang, Y.C.; et al. Granite-bauxite provenance of abnormally enriched boehmite and critical elements (Nb, Ta, Zr, Hf and Ga) in coals from the Eastern Surface Mine, Ningwu Coalfield, Shanxi Province, China. *J. Geochem. Explor.* **2022**, *239*, 107016. [CrossRef]
16. Ikeh, T.J.; Sun, B.L.; Liu, C.; Liu, Y.X.; Kong, Y.L.; Pan, X.Y. Modes of Occurrence and Enrichment of Trace Elements in Coal from the Anjialing Mine, Pingshuo Mining District, Ningwu Coalfield, Shanxi Province, China. *Minerals* **2022**, *12*, 1082. [CrossRef]
17. Zhou, M.X.; Dai, S.F.; Wang, X.B.; Zhao, L.; Nechaev, V.P.; French, D.; Graham, I.T.; Zheng, J.T.; Wang, Y.; Dong, M.J. Critical element (Nb-Ta-Zr-Hf-REE-Ga-Th-U) mineralization in Late Triassic coals from the Gaosheng Mine, Sichuan Basin, southwestern China: Coupled effects of products of sediment-source-region erosion and acidic water infiltration. *Int. J. Coal Geol.* **2022**, *262*, 104101. [CrossRef]

18. Sun, B.L.; Liu, Y.X.; Tajcmanova, L.; Liu, C.; Wu, J. In-situ analysis of the lithium occurrence in the No.11 coal from the Antaibao mining district, Ningwu Coalfield, northern China. *Ore Geol. Rev.* **2022**, *144*, 104825. [CrossRef]
19. Zhao, L.; Ward, C.R.; French, D.; Graham, I.T.; Dai, S.F.; Yang, C.; Xie, P.P.; Zhang, S.Y. Origin of a kaolinite-NH_4-illite-pyrophyllite-chlorite assemblage in a marine-influenced anthracite and associated strata from the Jincheng Coalfield, Qinshui Basin, Northern China. *Int. J. Coal Geol.* **2018**, *185*, 61–78. [CrossRef]
20. Zhao, L.; Dai, S.F.; Nechaev, V.P.; Nechaeva, E.V.; Graham, I.T.; French, D. Enrichment origin of critical elements (Li and rare earth elements) and a Mo-U-Se-Re assemblage in Pennsylvanian anthracite from the Jincheng Coalfield, southeastern Qinshui Basin, northern China. *Ore Geol. Rev.* **2019**, *115*, 103184. [CrossRef]
21. Wang, X.M.; Wang, X.M.; Pan, Z.J.; Yin, X.B.; Chai, P.C.; Pan, S.D.; Yang, Q. Abundance and distribution pattern of rare earth elements and yttrium in vitrain band of high-rank coal from the Qinshui basin, northern China. *Fuel* **2019**, *248*, 93–103. [CrossRef]
22. Hou, Y.H.; Liu, D.N.; Zhao, F.H.; Zhang, S.Q.; Zhang, Q.; Emmanuel, N.N.; Zhong, L.H. Mineralogical and geochemical characteristics of coal from the Southeastern Qinshui Basin: Implications for the enrichment and economic value of Li and REY. *Int. J. Coal Geol.* **2022**, *264*, 104136. [CrossRef]
23. *ASTM-D7582-2015*; Standard Test Method for Proximate Analysis of Coal and Coke by Macro Thermogravimetric Analysis. ASTM International: West Conshohocken, PA, USA, 2015.
24. *GB/T 214-2007*; Determination of Total Sulfur in Coal. (in Chinese). Standardization Administration of China: Beijing, China, 2007.
25. *GB/T 215-2003*; Determination of Forms of Sulfur in Coal. (in Chinese). Standardization Administration of China: Beijing, China, 2003.
26. *GB/T 15224.1-2018*; Classification for Quality of Coal-Part 1: Ash. (in Chinese). Standardization Administration of China: Beijing, China, 2018.
27. *GB/T 15224.2-2010*; Classification for Quality of Coal-Part 2: Sulfur Content. (in Chinese). Standardization Administration of China: Beijing, China, 2010.
28. Dai, S.F.; Ren, D.Y.; Chou, C.L.; Finkelman, R.B.; Seredin, V.V.; Zhou, Y.P. Geochemistry of trace elements in Chinese coals: A review of abundances, genetic types, impacts on human health, and industrial utilization. *Int. J. Coal Geol.* **2012**, *94*, 3–21. [CrossRef]
29. Dai, S.F.; Seredin, V.V.; Ward, C.R.; Hower, J.C.; Xing, Y.W.; Zhang, W.G.; Song, W.J.; Wang, P.P. Enrichment of U-Se-Mo-Re-V in coals preserved within marine carbonate successions: Geochemical and mineralogical data from the Late Permian Guiding Coalfield, Guizhou, China. *Miner. Dep.* **2015**, *50*, 159–186. [CrossRef]
30. Ketris, M.P.; Yudovich, Y.E. Estimations of Clarkes for Carbonaceous biolithes: World averages for trace element contents in black shales and coals. *Int. J. Coal Geol.* **2009**, *78*, 135–148. [CrossRef]
31. Grigoriev, N.A. *Chemical Element Distribution in the Upper Continental Crust*; (in Russian). UB RAS: Ekaterinburg, Russia, 2009.
32. Dai, S.F.; Li, D.; Chou, C.L.; Zhao, L.; Zhang, Y.; Ren, D.Y.; Ma, Y.W.; Sun, Y.Y. Mineralogy and geochemistry of boehmite-rich coals: New insights from the Haerwusu Surface Mine, Jungar Coalfield, Inner Mongolia, China. *Int. J. Coal Geol.* **2008**, *74*, 185–202. [CrossRef]
33. Sun, Y.Z.; Li, Y.H.; Zhao, C.L.; Lin, M.Y.; Wang, J.X.; Qin, S.J. Concentrations of Lithium in Chinese Coals. *Energy Explor. Exploit.* **2010**, *28*, 97–104. [CrossRef]
34. Liu, B.J.; Wang, J.Y.; He, H.T.; Mishra, V.; Li, Y.H.; Wang, J.X.; Zhao, C.L. Geochemistry of Carboniferous coals from the Laoyaogou mine, Ningwu coalfield, Shanxi Province, northern China: Emphasis on the enrichment of valuable elements. *Fuel* **2020**, *279*, 118414. [CrossRef]
35. Sun, B.L.; Zeng, F.G.; Moore, T.A.; Rodrigues, S.; Liu, C.; Wang, G.Q. Geochemistry of two high-lithium content coal seams, Shanxi Province, China. *Int. J. Coal Geol.* **2022**, *260*, 104059. [CrossRef]
36. Dai, S.F.; Jiang, Y.F.; Ward, C.R.; Gu, L.D.; Seredin, V.V.; Liu, H.D.; Zhou, D.; Wang, X.B.; Sun, Y.Z.; Zou, J.H.; et al. Mineralogical and geochemical compositions of the coal in the Guanbanwusu Mine, Inner Mongolia, China: Further evidence for the existence of an Al (Ga and REE) ore deposit in the Jungar Coalfield. *Int. J. Coal Geol.* **2012**, *98*, 10–40. [CrossRef]
37. Dai, S.F.; Ren, D.Y.; Chou, C.L.; Li, S.S.; Jiang, Y.F. Mineralogy and geochemistry of the No. 6 coal (Pennsylvanian) in the Junger Coalfield, Ordos Basin, China. *Int. J. Coal Geol.* **2006**, *66*, 253–270. [CrossRef]
38. Dai, S.F.; Zou, J.H.; Jiang, Y.F.; Ward, C.R.; Wang, X.B.; Li, T.; Xue, W.F.; Liu, S.D.; Tian, H.M.; Sun, X.H.; et al. Mineralogical and geochemical compositions of the Pennsylvanian coal in the Adaohai Mine, Daqingshan Coalfield, Inner Mongolia, China: Modes of occurrence and origin of diaspore, gorceixite, and ammonian illite. *Int. J. Coal Geol.* **2012**, *94*, 250–270. [CrossRef]
39. Dai, S.F.; Li, T.J.; Jiang, Y.F.; Ward, C.R.; Hower, J.C.; Sun, J.H.; Liu, J.J.; Song, H.J.; Wei, J.P.; Li, Q.Q.; et al. Mineralogical and geochemical compositions of the Pennsylvanian coal in the Hailiushu Mine, Daqingshan Coalfield, Inner Mongolia, China: Implications of sediment-source region and acid hydrothermal solutions. *Int. J. Coal Geol.* **2015**, *137*, 92–110. [CrossRef]
40. Dai, S.F.; Finkelman, R.B.; French, D.; Hower, J.C.; Graham, I.T.; Zhao, F.H. Modes of occurrence of elements in coal: A critical evaluation. *Earth-Sci. Rev.* **2021**, *222*, 103815. [CrossRef]
41. Finkelman, R.B.; Palmer, C.A.; Wang, P.P. Quantification of the modes of occurrence of 42 elements in coal. *Int. J. Coal Geol.* **2018**, *185*, 138–160. [CrossRef]
42. Wang, W.F.; Qin, Y.; Liu, X.H.; Zhao, J.L.; Wang, J.Y.; Wu, G.D.; Liu, J.T. Distribution, occurrence and enrichment causes of gallium in coals from the Jungar Coalfield, Inner Mongolia. *Sci. China Earth Sci.* **2011**, *54*, 1053–1068. [CrossRef]

43. Seredin, V.V.; Dai, S.F. Coal deposits as potential alternative sources for lanthanides and yttrium. *Int. J. Coal Geol.* **2012**, *94*, 67–93. [CrossRef]
44. Taylor, S.R.; McLennan, S.M. *The Continental Crust: Its Composition and Evolution*; Blackwell: Oxford, UK, 1985; p. 312.
45. Dai, S.F.; Graham, I.T.; Ward, C.R. A review of anomalous rare earth elements and yttrium in coal. *Int. J. Coal Geol.* **2016**, *159*, 82–95. [CrossRef]
46. Wang, W.F.; Qin, Y.; Sang, S.X.; Zhu, Y.M.; Wang, C.Y.; Weiss, D.J. Geochemistry of rare earth elements in a marine influenced coal and its organic solvent extracts from the Antaibao mining district, Shanxi, China. *Int. J. Coal Geol.* **2008**, *76*, 309–317. [CrossRef]
47. Finkelman, R.B.; Dai, S.F.; French, D. The importance of minerals in coal as the hosts of chemical elements: A review. *Int. J. Coal Geol.* **2019**, *212*, 103251. [CrossRef]